CHEMBIOCHEM

DOI: 10.1002/cbic.200800696

Fabrication of Carbohydrate Surfaces by Using Nonderivatised Oligosaccharides, and their Application to Measuring the Assembly of Sugar–Protein Complexes

Jonathan F. Popplewell,*[a] Marcus J. Swann,[a] Yassir Ahmed,[b] Jerry E. Turnbull,[b] and David G. Fernig[b]

Surface-based tools, such as microarrays and optical biosensors, are being increasingly applied to the analysis of carbohydrate–protein interactions. A key to these developments is the presentation of the carbohydrate to the protein target. Dual polarisation interferometry (DPI) is a surface-based technique that permits the real-time measurement of the changes in thickness, refractive index and mass of adsorbates 100 nm thick or less on the surface of a functionalised waveguide. DPI has been used to design and characterise a surface on which the orientation and density of the immobilised carbohydrates is suitable for studying their interactions with proteins and where nonspecific binding is reduced to less than 5% of total binding. A thiol-functionalised surface was derivatised with a heterobifunctional crosslinker to yield a hydrazide surface. This was treated with oligosaccharides, derived from keratan sulfate (KS) chondroitin sulfate (CS) and heparin, that possess a reducing end. To block the unreacted hydrazide groups, the surface was treated with an aldehyde-functionalised PEG. The heparin DP-10 surfaces were then used to determine the performance of the immobilised DP-10 with respect to binding of two well-characterised proteins, lactoferrin (Lf) and fibroblast growth factor-2. The results show that Lf could adopt two different orientations, at high protein loadings the protein layer thickness corresponded to an "end-on" orientation of Lf, whilst rinsing with buffer saw the Lf molecules adopt a "side-on" configuration. In the case of FGF-2, a single monolayer of protein bound to DP-10 was observed. These results demonstrate that the new surface can be used to resolve key questions relating to the binding of proteins to carbohydrates, including, when used in DPI, the resolution of the geometry of complexes, an area that is frequently controversial.

Introduction

Due to the large number of saccharide building blocks and the variety of linkages between them, glycans have an enormous potential to carry information, far exceeding that of nucleic acids or proteins.[1] In animals, this information space has been exploited in the regulation of cell–cell communication, with the glycans of the cell surface and pericellular matrix intimately involved in the regulation of virtually all aspects of cell–cell communication. For example, over 250 extracellular regulatory proteins in humans have been documented to bind to the glycosaminoglycans heparin and heparan sulfate, and these interactions modulate the activities of these proteins.[2]

The synthesis of carbohydrates is not template-driven, and their structural complexity combines to make the elucidation of their functions extremely challenging. This has led to the development of new tools and techniques for this purpose. Examples include new sequencing strategies,[3,4] spectroscopic analysis of conformation[5,6] and the increasing application of a range of sensitive surface-based techniques, such as glycoarrays[7,8] and optical biosensors.[9] These surface-based approaches are attractive, since they afford sensitivity and the potential for the high-throughput analysis of interactions.

A key challenge in fabricating carbohydrate surfaces is the establishment of reliable and reproducible chemistries for the immobilisation of the oligosaccharides onto a solid substrate while retaining their functionality. A number of different strategies have been employed to immobilise carbohydrates on surfaces. One approach is simply noncovalent adsorption of negatively charged glycosaminoglycans on positively charged surfaces,[10] but this has the obvious drawback that binding sites on the sugar might be obscured and the underlying surface might present adventitious binding sites for the basic patches on proteins that commonly interact with this class of polysaccharides. Alternatively derivatised oligosaccharides have been used, for example carbohydrate chips have been prepared by the Diels–Alder-mediated immobilisation of carbohydrate–cyclopentadiene conjugates to self-assembled monolayers that present benzoquinone and penta(ethylene glycol) groups.[11] Other researchers have employed an alkyne-functionalised glass surface with the derivatised sugar attached by an azide coupling.[12] Attachment of oligosaccharides to thiol surfaces through the formation of mercury–sugar adducts[13] has been performed with the addition of mercury to the non-

[a] Dr. J. F. Popplewell, Dr. M. J. Swann
Farfield Group, Ltd., Farfield House
Electra Way, Crewe CW1 6GU (UK)
Fax: (+44) 870-950-9718
E-mail: jpopplewell@farfield-group.com

[b] Y. Ahmed, Prof. J. E. Turnbull, Prof. D. G. Fernig
School of Biological Sciences, University of Liverpool
Crown Street, Liverpool L69 3BX (UK)

reducing end of heparin oligosaccharides produced by lyase digestion. Maleimide-functionalised sugars have been attached to thiol surfaces,[14] and the opposite route of thiol-functionalised sugar addition to maleimide surfaces has also been utilised.[15,16] Other amine chemistry strategies have involved coupling amine-functionalised sugars to *N*-hydroxysuccinimide (NHS) surfaces[17] or reductive amination of aldehydes on amine-functionalised surfaces.[18] A commonly employed modification is the biotinylation of heparin at different parts of the heparin molecule, namely coupling through either carboxylate groups or unsubstituted amines along the heparin chain or through the reducing terminus of oligosaccharide heparin chains.[9,19–21] The results of these studies suggest that the route of heparin biotinylation could significantly affect the binding of proteins.[22]

We have developed an oligosaccharide-immobilisation strategy for orientated coupling of oligosaccharides. This strategy incorporates the direct immobilisation of oligosaccharides through their reducing ends onto a hydrazide-functionalised surface and the blocking of unreacted hydrazides with an aldehyde-functionalised poly(ethylene glycol) (PEG-CHO). By monitoring the progress in real-time by dual-polarisation interferometry (DPI), it was possible to determine, at each step, the density and orientation of the groups attached to the surface. Surfaces with oligosaccharides derived from a range of glycosaminoglycans were prepared: heparin, keratan sulfate (KS) and chondroitin sulfate (CS). Surfaces prepared with a decasaccharide (degree of polymerisation 10; DP-10) from heparin were then analysed in detail with respect to the binding of lactoferrin and fibroblast growth factor-2 by using dual-polarisation interferometry. The data show that binding of these proteins is compatible with the known structures of their complexes with glycosaminoglycans and, furthermore, that FGF-2 only forms monomers on these oligosaccharides.

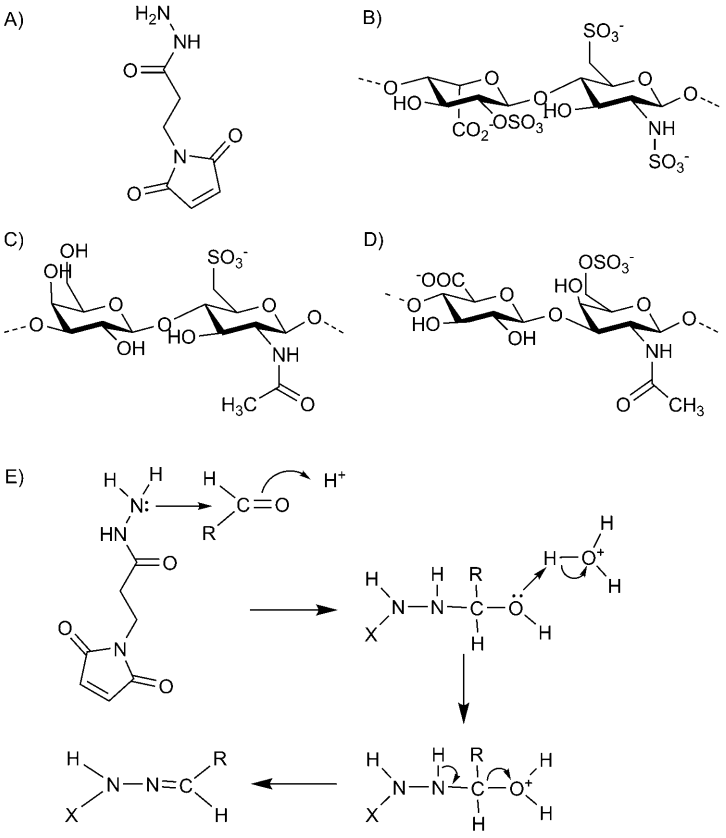

Scheme 1. A) The heterobifunctional crosslinker *N*-[β-maleimidopropionic acid] hydrazide, trifluoroacetic acid salt (BMPH). B) The predominant repeating structure of a heparin decasaccharide obtained by nitrous acid scission can be represented by UA(2S)–$[GlcNS6S–IdoA2S]_4$-$AMann_R6S$, where UA = uronic acid residue and AMannR = anhydromannose residue. The basic heparin disaccharide repeat unit of GlcNS6S–IdoA2S is displayed as (B). C) The basic repeat unit of keratan sulfate, *N*-acetylglucosamine and galactose. D) The basic repeat structure of chondroitin sulfate, glucuronate and *N*-acetylgalactosamine. E) Complete coupling reaction for BMPH with a reducing sugar.

Results and Discussions

Quantifying covalent coupling of linker and oligosaccharides to the surface

The thiol surface was modified by the sulfhydryl-reactive heterobifunctional crosslinker BMPH (Scheme 1 A) to yield aldehyde-reactive terminal hydrazide functional groups. The hydrazide functional group displayed on the surface can then efficiently react with the reducing end of the oligosaccharide (Scheme 1 B), with the sugar displayed in a predictable orientation. The mechanism for the coupling reaction is given in Scheme 1 E.

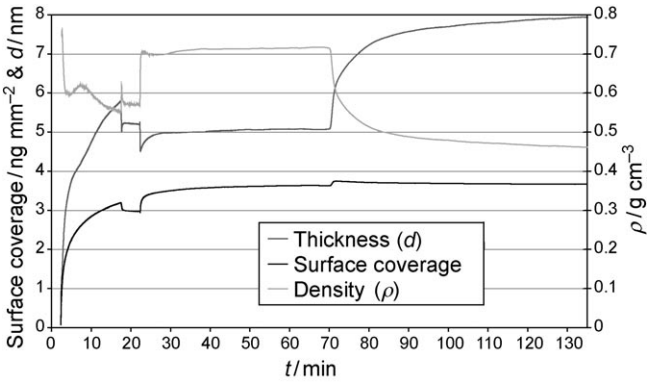

Figure 1. Changes in surface coverage and dimensions of BMPH and heparin as the oligosaccharide surface is formed. The BMPH linker was added at ca. $t = 3$ min, and, following PBS washing, the heparin was added at 21 min. After 70 min, the surface was washed with PBS.

The assembly of the BMPH linker and subsequent oligosaccharide layer can be followed in real-time; a typical reaction profile is shown in Figure 1. The BMPH linker was added at 3 min and, following PBS washing ($t = 17$ min), formed a layer with a surface coverage of 3.0 ng mm^{-2} and a thickness measured at 5.2 nm. The addition of oligosaccharide was started at 21 min; upon addition of the heparin solution the change in pH from 7.4 to 5 causes the measured thickness of the layer to

decrease and the measured density to increase, an effect of the bulk refractive index change. From 20 to 70 min the heparin was observed to bind, gradually increasing the surface coverage. At 70 min, the flow cells were washed with PBS at pH 7.4, which reverses the bulk shift seen upon injection of the heparin-derived oligosaccharide ($t = 20$ min). From the start of the heparin injection there is an increase in thickness from 5.0 nm to 7.9 nm, which represents the increase in thickness induced by the binding of heparin to the linker. The average density of the combined BMPH and heparin layer is lower after the binding of the oligosaccharide. An increase in density might be expected if the carbohydrate had inserted in between the linker molecules, but, as observed from Figure 1, the average density of the combined BMPH and heparin layers is lower after the binding of the heparin. This observation, coupled with the significant thickness increase upon heparin binding clearly shows the heparin has bound above the plane of the BMPH substructure and is thus sterically available to bind to proteins.

Surface coverage and orientation measurements

It has been established that a crucial feature of heparin is the minimal length for ligand binding and activity, with heparin-derived tetrasaccharides found to be sufficient to interact with FGF-2, but DP-10–12 required for optimising the proliferative activity of FGF-2.[9] Thus, of critical importance in surface-based studies examining such interactions is the orientation and thus availability of the protein binding structures within the polysaccharide. For a series of immobilisations the average surface coverage values of DP-10 (taking the refractive index increment, RII, of DP-10 to be 0.138 $cm^3 g^{-1}$)[23] were measured at (0.89 ± 0.48) ng mm^{-2}, and the corresponding thickness values (d) measured at (1.63 ± 0.46) nm. From NMR studies of heparin-derived oligosaccharides, a fully extended DP-10 chain perpendicular to the surface linker would expect to show a thickness increase of 4 nm, based on the disaccharide units having a length of 0.8 nm,[24] and an orientation parallel to the surface (heparin lying on the linker) would expect to show an increase in thickness of 0.9 nm (PDB ID: 1HPN). Therefore, we can conclude that the orientation of the oligosaccharide is likely to be at an acute angle to the surface, but critically not lying flat on the linker and so available for binding protein partners.

This data series was compared with a smaller series ($n = 3$) of DP-4 immobilisations, which showed a near identical average surface coverage value, (0.89 ± 0.16) ng mm^{-2}, and similar thickness values of (1.45 ± 0.61) nm. It seems likely that by adopting an acute angle to the surface, the longer DP-10 might have blocked further BMPH sites from reaction; in contrast, the shorter DP-4 undergoes much less interaction with the surface and has a more perpendicular orientation.

The reaction of oligosaccharides and hydrazide was observed to proceed more fully at pH 5 than at pH 7, as a surface coverage of 1.06 ng mm^{-2} was obtained at pH 4.9 compared to only 0.56 ng mm^{-2} at pH 7.4 after the same reaction time and on the same surface coverage of BMPH linker. This increased amount of oligosaccharide binding at pH 5 is to be expected as the reaction between a hydrazide and reducing terminus of a sugar is a nucleophilic addition–elimination reaction. The hydrazide first adds across the carbon–oxygen double bond of the sugar, with this addition taking place at a faster rate if the carbonyl carbon is more electron deficient, induced by increased protonation at lower pH values. As none of the carboxylate or sulfate groups of the oligosaccharide are involved in the reaction with the hydrazide, it is unlikely that a change in their charge status affects the extent of this reaction.

The KS oligosaccharide, $M_W = 5000$–8000, added at the same concentration and pH as the heparin oligosaccharides gave consistently higher surface coverages, (1.28 ± 0.68) ng mm^{-2}, whilst the CS oligosaccharide, with a similar chain length to KS, had much lower coverage values of (0.63 ± 0.29) ng mm^{-2}. As for the reaction of heparin with hydrazide, reactions between KS and linker and CS and linker are nucleophilic addition–elimination reactions with none of the carboxylate or sulfate groups of the oligosaccharide involved in the reaction with the hydrazide. As can be seen from Scheme 1 C, keratan sulfate is composed of repeating units of galactose and *N*-acetylglucosamine, whilst chondroitin sulfate is composed of repeating units of glucuronate and *N*-acetylgalactosamine sulfate (Scheme 1 D). The difference in reactivity between KS and CS with hydrazide might be caused by the sugar residues adjacent to the reducing end affecting the reactivity towards the hydrazide. The degree of sulfonation and carboxylation along the oligosaccharide chain is unlikely to affect the reactivity of the reducing terminus with the hydrazide linker.

The measured thickness of the CS oligosaccharide layers, (0.71 ± 0.33) nm, suggests a flat orientation, one in which the CS is parallel to the hydrazide layer, whereas the thickness of the KS layer is higher at (1.38 ± 1.21) nm. One explanation for this observation is that the higher charge density of the CS oligosaccharide compared to the KS, due to the carboxylate group per disaccharide (as can be seen in Scheme 1), means that the CS disaccharide repeat unit has an average charge level of at least two. This might result in a thinner layer, most probably due to the greater electrostatic interaction with the positively charged amine groups (on the linker) on the surface, which would force an orientation more parallel to the surface. In contrast, the absence of carboxylate on KS means that the average charge level per disaccharide repeat unit is less at 1.3–1.5 (all the GlcNAc are sulfated and $^1/_2$ to $^1/_3$ galactoses are sulfated) and might allow the KS layer to be more perpendicular to the surface. However, the greater thickness observed with the heparin DP-4 and DP-10, at about 1.5 nm, which carry a higher charge per disaccharide (3 sulfates, 1 carboxylate) argues against this interpretation and suggests that some non-electrostatic interactions with the underlying surface and or solvent are predominantly responsible for determining the orientation of the immobilised sugars.

It is possible for negatively charged molecules such as oligosaccharides to adsorb nonspecifically through electrostatic interactions to the positively charged hydrazide surface. In order to show that the oligosaccharides were covalently attached rather than nonspecifically adsorbed, the surface was washed with 75 flow cell exchanges of 2 M NaCl. Comparison of both

the mass and orientation (thickness) of the oligosaccharide layer, pre and post the 2 M NaCl challenge, in other words while the surface is being perfused with PBS and 2 M NaCl is not present, showed that there was no detectable change in either of these parameters. Thus the oligosaccharides are covalently attached to the surface and not attached by electrostatic interactions, with the reported thicknesses of the oligosaccharide layers being those in the absence of high salt.

A key advantage of attaching the oligosaccharides by using the route described here is that the sugar is covalently attached to the surface via the reducing end and, with the exception of the CS oligosaccharide, the sugars are not interacting directly with the surface and are thus readily available for binding to proteins.

Covalent coupling of PEG-aldehyde on unreacted hydrazide sites/Minimising nonspecific adsorptions of proteins

As with all surfaces, nonspecific adsorption is a potential major problem. At a high density of oligosaccharide immobilised on the surface, the nonspecific binding of a number of proteins was markedly reduced. For example, an immobilised KS surface coverage of 1.40 ng mm^{-2} showed nearly no nonspecific binding to concanavalin (Con A; which only binds α-mannose and α-glucose) or bovine serum albumin (BSA), whilst other surfaces where the oligosaccharide surface coverage was deliberately reduced (by simply reducing the time for which the KS oligosaccharide was incubated on the BMPH linker) to create a surface oligosaccharide coverage <0.5 ng mm^{-2} showed significant nonspecific binding of Con A.

A number of reasons indicated that a blocking step was necessary after the coupling of the oligosaccharide to the surface. Firstly, at high ligand coverage, adjacent sugar chains can sterically hinder protein binding or contribute to new, multioligosaccharide binding sites, thus disturbing measured kinetic and thermodynamic binding parameters. Secondly, not all sugars (e.g., CS) could be immobilised at sufficient coverage to ensure no detectable nonspecific binding. Thirdly, certain proteins, such as lactoferrin and fibroblast growth factor-2 (FGF-2), were observed to show significant nonspecific binding to the underlying hydrazide layer (data not shown). Initial blocking strategies involved using BSA, which did prove effective, but the use of a protein-blocking agent raises concerns about protein–protein interactions and the longevity of an oligosaccharide surface containing protein.

Use of poly(ethylene glycol) as a blocking agent has found a number of applications.[25–27] Indeed, in our previous studies, we demonstrated that glycoarrays can be prepared by using hydrazide-modified surfaces on which nonspecific binding is reduced by the use of PEG-aldehyde blocking agent.[28] However, surface characterisation of these arrays has not been performed. Therefore, a short-chain PEG with a reducing end to react with unreacted hydrazide was employed as a blocking agent (Figure 2). The CHO-PEG reacted with free hydrazide sites remaining after sugar immobilisation, and this rate of reaction can be compared with the control (100% PEG) flow cell not treated with carbohydrate (Figure 2).

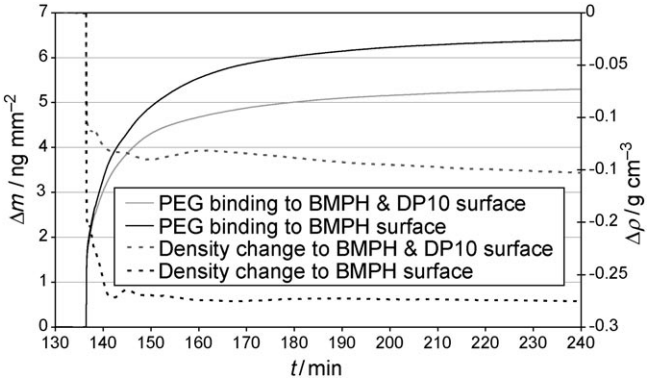

Figure 2. Changes in surface coverage upon PEG-CHO binding. The increase in surface coverage was determined for the non-heparin-treated surface (black line) and compared to that of the BMPH surface already treated with DP-10 (grey line). The dense linker layer undergoes a greater decrease in density (right-hand axis) upon binding CHO-PEG than the less-dense BMPH–carbohydrate surface.

By examining how much PEG-CHO binds after the oligosaccharide addition, the number of free hydrazide groups can be related to the measured oligosaccharide thickness. By using the mass of BMPH bound, the maximum amount of PEG-CHO that would bind to a 100% active surface can be estimated, assuming that BMPH and PEG-CHO interact in a 1:1 manner. Typically the amount of immobilisation of PEG-CHO is 40–50% ($n>10$) of the maximum that could bind to a BMPH surface. In other words, the packing density and/or activity of BMPH only permit reaction with about 50% of the hydrazide sites. Working on the same 1:1 basis for BMPH reacting with oligosaccharide, the typical coverage of oligosaccharide is 1–5% of the theoretical maximum coverage for a BMPH surface. Taking the example in Figure 1, the mass of DP-10 bound is 2% of the expected maximum value, assuming all the hydrazide molecules are orientated and available for reaction. The level of binding of PEG-CHO around the DP-10 to the remaining hydrazide sites is 5.3 ng mm^{-2}, which equates to 39% of the theoretical maximum. The mass of PEG-CHO binding to the BMPH after treatment with DP-10 was compared to that observed on a BMPH surface not treated with DP-10. Again, by using the surface in Figure 2 as the example, 6.4 ng mm^{-2} of PEG-CHO is observed to bind to the control (non DP-10) channel, which equates to 45% of the theoretical maximum. Thus, in the absence of sugar, only 6% greater coverage of PEG-CHO is obtained. Therefore, broadly the same amount of PEG-CHO reacts with BMPH whether or not it has been treated with DP-10. This adds further evidence to the measured thickness values for DP-10 that the sugar is not blocking the hydrazide and is thus in a nonplanar orientation.

Examining the assembly of protein–oligosaccharide complexes

Interaction with lactoferrin: The interaction of lactoferrin with the oligosaccharide surfaces was characterised to validate the surfaces for the analysis of protein–sugar interactions. Synthesised by mucosal epithelium, lactoferrin is an inflammatory re-

sponse protein and is known to have activities as diverse as scavenging iron and inhibiting bone marrow formation.[29,30] It is known to bind to anionic polysaccharides including heparin.[31–33] The unit cell dimensions for bovine lactoferrin (bLf) are given as 13.9×8.7×7.3 nm,[34] and the protein has a reported pI in the pH range of 8. The amino acid sequence of bovine lactoferrin consists of a single polypeptide chain of 689 residues[35,36] folded into two lobes (Figure 3), the N-lobe and the C-lobe (representing the N- and C-terminal halves of the protein[34]). The N- and C-lobes are linked by a three-turn helix, with the polypeptide chain essentially identical to that of human lactoferrin. Whilst the physical and biochemical properties of human lactoferrin have been well investigated, the lactoferrins of other animals have had less study. It has been proposed that the N-terminal region of lactoferrin is responsible for heparin binding, through the sequence BXBB, where B denotes positively charged amino acids. Analysis of proteolytic digests of lactoferrin have identified four sets of amino acid residues that bind to heparin, 1–10, 17–31, 22–31 and 32–41.[37] However, analysis of the heparin-binding properties of the entire protein have not been reported, and, whilst the data presented here cannot give any new information on the specificity of the interaction, the negatively charged oligosaccharide surface and DPI have been used to probe the dimensional changes that occur when bLf binds to heparin-derived oligosaccharides.

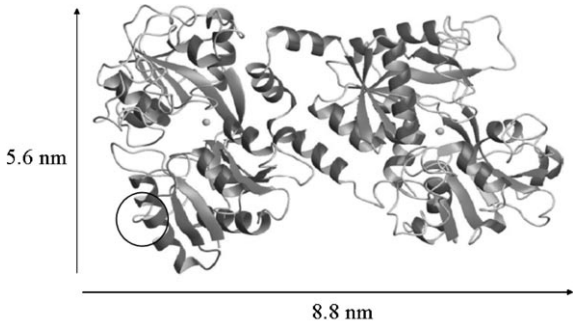

Figure 3. Ribbon diagram of bovine lactoferrin, with the ringed area the region for the sequence of amino acids postulated to bind heparin (PDB ID: 1blf).

Above a threshold concentration, the measured increased in thickness for the addition of Lf to DP-10 is 8.5–10 nm (Figure 4). This is consistent with bLf binding through basic residues to form a monolayer in an "end-on" configuration, and with reports that used AFM to examine lactoferrin adsorbing on contact lens material, where a significant number of lactoferrin molecules were adsorbed in an "end-on" configuration.[38]

When the lactoferrin layer is washed with running buffer, it is observed that, on average, 50% of the lactoferrin dissociates and the remaining 50% now has a thickness of 5.8 nm, indicative of Lf adopting a "side-on" configuration. Thus high surface concentrations of protein force lactoferrin into an "end-on" orientation, perhaps due to geometrical constraints, lactoferrin then adopts a "side-on" configuration when the surface bLf packing density is decreased upon PBS washing. It is not clear if the population of "end-on" orientated lactoferrin molecules are desorbed leaving only the "side-on" population present or if, during the desorption of lactoferrin from the "end-on" configuration, some molecules rock over or reattach in the "side-on" configuration.

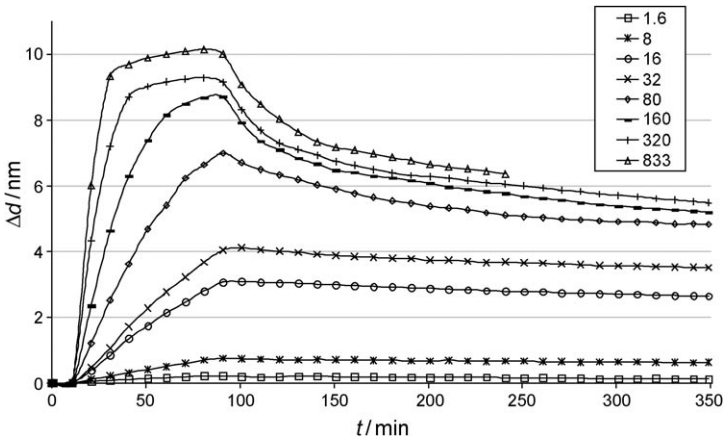

Figure 4. Changes in thickness observed upon binding of different concentrations of lactoferrin to a DP-10 surface. Increasing concentrations of lactoferrin (given in nM) were allowed to flow over the DP-10 surface. From the change in thickness it can be inferred that the Lf molecules adopt an "end-on" configuration whilst protein is flowing over the chip, then, as the surface is washed (at $t = 90$ s), some of the Lf desorbs with the remaining Lf on average in the "side-on" configuration. Injections at 32 nM and below are observed to be mass-transport limited.

Whilst the data here cannot categorically rule out multiple layers of lactoferrin being responsible for the protein thickness layers observed at 8.5–10 nm, there are two supporting pieces of data that strongly suggest that the two thicknesses observed represent a monolayer of lactoferrin in two different orientations. The first significant piece of evidence to support the hypothesis comes from the lack of multiplies of the thickness of a "side-on" configuration. A multilayer of lactoferrin molecules in the "side-on" configuration would be expected to have a thickness of at least 2×5.8 nm, whereas the maximum thickness observed by DPI does not exceed 10 nm, a value much more consistent with lactoferrin in an "end-on" configuration.

The second comes from a comprehensive study of lactoferrin absorption on glass as measured by AFM.[38] These authors reported that one monolayer of lactoferrin per surface adsorbs, and increasing the concentration to 1.0 mg mL^{-1} (14 μM) does not give rise to a thicker layer. The authors also reported that lactoferrin adopts both "side-on" and "end-on" configurations. The authors described how a significant number of lactoferrin molecules are adsorbed in an "end-on" configuration and that it is the α-helix joining the two lobes that is being compressed under the load of the AFM probe.

The data in Figure 4 represent a typical data set with two clear orientations. On some of the oligosaccharide surfaces

thickness increases upon addition of Lf corresponded to slightly thicker values than a monolayer of lactoferrin in an "end-on" configuration, and equally some measured in the "side-on" configuration showed about 10% variation from 5.8 nm. The orientation of lactoferrin on carbohydrate will be determined by a number of factors, including electrostatic and van der Waals interactions between the sugar and lactoferrin, and the energy gains associated with conformational change of molecules as they bind. Thus, whilst not all the thickness values observed for the two orientations corresponded exactly to the dimensions of the "end-on" and "side-on" configurations, each surface tested showed a set of measurements close to "end-on" dimensions at 8.8 nm and a switch to a set of "side-on" dimensions at 5.8 nm.

On all the surfaces tested, the addition of 2 M NaCl fully regenerated the surface (< 5% protein remaining), and in all cases the amount of bLf binding to the control (PEG only) channel was < 5% of that observed with the oligosaccharide with PEG surface.

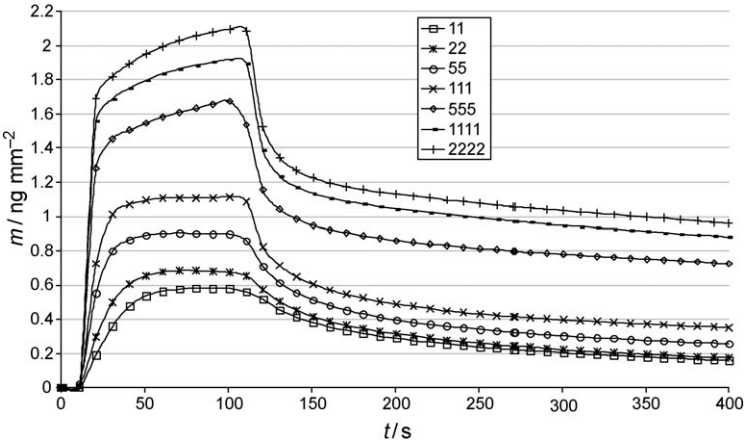

Figure 5. Binding curves of lactoferrin (in ng mm^{-2}) at various concentrations to immobilised DP-10. Lactoferrin was diluted to various concentrations (nM) and injected over the DP-10. Following injection, the protein solution was replaced with running buffer (PBS) to monitor dissociation kinetics and the structure of the 2D complex in buffer solution.

Affinity of lactoferrin for heparin: Titration of tritium-labelled pig mucosal heparin ($M_W = 15$ kDa) indicated approximately five binding sites for lactoferrin per heparin chain,[39] thus full-length heparin cannot be fitted with a 1:1 binding model.[22] A molecular weight of 15 kDa corresponds to about 30 disaccharides, and, if there are five binding sites per chain, it seems reasonable to assume there is one Lf binding site for six disaccharides (DP-12). Since the reducing sugar of the immobilised DP-10 is unlikely to be free for interaction with protein, DP-10 will be a reasonable model system to fit with 1:1 stoichiometry (Figure 5).

Analysis of the binding observed between lactoferrin and DP-10 at equilibrium produced a K_d of 87 ± 42 nM from a non-linear regression fit to Scatchard-transformed data. Kinetic analysis delivered an average association rate constant, k_{ass} of 2.9×10^5 M^{-1} s^{-1} and an average k_{diss} of 4.5×10^{-2} s^{-1} and hence a kinetically determined value of K_d of 150 ± 35 nM. The K_d values determined from the analysis of binding at equilibrium and from the kinetic parameters are equivalent; this indicates that the data are self-consistent. Moreover, these K_d values are in agreement with that of 99 ± 35 nM determined from analysis of the binding of bLf to glycosaminoglycans on human the carcinoma cell line HT29.[40]

Heparin surfaces binding FGF-2 (bFGF): The fibroblast growth factors (FGFs) are the archetypal heparan-sulfate-binding growth factors. FGF-2 has been shown to bind to tetrasaccharides derived from heparin, and these have been shown to be sufficient for the activation of the FGF receptor, though DP-8 has been found to the minimum size required for optimal activation of cellular signalling and proliferation.[9] With heparan-sulfate-derived oligosaccharides, DP-8 is the minimum length required for activity,[41] and crystal structures of FGF-2 with heparin-derived DP-4 and DP-6 indicate a 1:1 association. However cocrystals of FGF ligand, FGF receptor and oligosaccharides demonstrate two very different organisations of the complex, whereas analysis of complexes by gel filtration, indicates that the growth factor can dimerise on the sugar, which requires oligosaccharides of ~DP-8.[42] The oligosaccharide surfaces developed here provide a means to analyse the dimensions of a FGF-2 layer on DP-10, and thus establish quantitatively whether the sugar does indeed oligomerise the growth factor.

Additions of FGF-2 were made in the range 2.36–1180 nM FGF-2, with FGF-2 appearing to saturate the surface over the range 236–1180 nM. At high concentrations of FGF-2, the protein layer on the DP-10 surface had a thickness of (4.11 ± 0.11) nm ($n = 3$; Figure 6). Based on comparison with the unit cell parameters of FGF-2, $3.09 \times 3.34 \times 3.59$ nm,[43] the measured layer thickness increase upon addition of FGF-2 to DP-10 shows unambiguously that FGF-2 forms a diffuse monolayer under these conditions, where the stoichiometry is FGF-2/DP-10 0.14:1. Therefore, whilst we cannot rule out the presence of *trans* dimers of FGF-2 on the DP-10, this seems very unlikely given the substoichiometric ratio of FGF-2 to DP-10 and the complete absence of any data to suggest that the FGF-2 interaction with the sugar is in any way cooperative, despite many

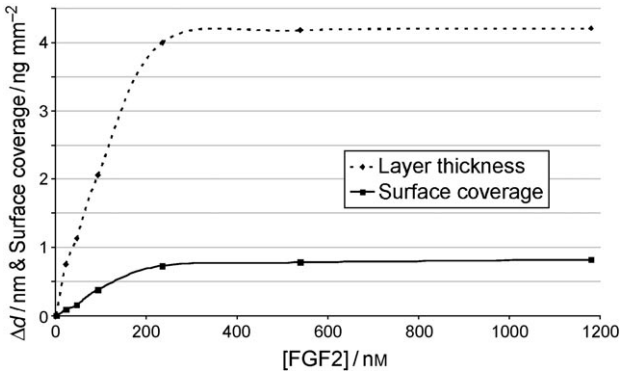

Figure 6. The changes in thickness and surface coverage were measured for FGF-2 binding to a DP-10 surface.

years of intensive biophysical analysis. This conclusion is supported directly by the thickness data, which show clearly that binding of FGF-2 causes an increase in thickness of 4.11 nm, which can only be accounted for by the FGF-2 binding on the "top" side of the DP-10.

Kinetic analysis delivered rate constants of $k_{ass} = 1.7 \times 10^5\ M^{-1}s^{-1}$ and $k_{diss} = 9.4 \times 10^{-3}\ s^{-1}$ and hence a kinetically determined value of $K_d = 57$ nM, similar to that measured previously by kinetic and equilibrium analysis.[9]

Conclusions

Oligosaccharide surfaces have been produced where the sugar is immobilised through its reducing end, and has been shown to be oriented towards the solution rather than associated parallel to the underlying surface. Combined with the blocking of the surface with a short chain PEG, these surfaces present the sugars optimally to proteins, and are thus a valuable tool for the analysis of protein–sugar interactions. In this work DPI was used to probe the geometry of the protein–sugar complexes, and revealed new properties of the two test proteins: lactoferrin possesses two modes of association, whereas FGF-2 forms monomeric complexes with a heparin-derived DP-10. Given the very low nonspecific binding and excellent regenerability of these surfaces, and the fact that they can be produced with any sugar that has a reducing end, they should have wide applicability in the analysis of protein–sugar interactions by a range of surface techniques, from biophysics to microarrays.

Experimental Section

Materials: All chemical and biochemical products were of analytical grade. BSA, bLf, lectin from *Maackia amurensis* (MAA), Con A, lectin from *Triticum vulgaris*, phosphate-buffered saline tablets (PBS, pH 7.4), HEPES and NaCl were supplied by Sigma. BMPH (*N*-[β-maleimidopropionic acid]hydrazide, trifluoroacetic acid salt) was from Pierce (Cramlington, UK), whilst CH_3O-PEG-NH-CO-C_4H_8-CHO or "PEG-CHO" was obtained from Rapp Polymere GmbH (Tübingen, Germany). Human recombinant FGF-2 was produced and purified as described.[44] Waveguide chips modified with an alkoxysilylthiol layer were supplied by the Farfield Group Ltd (Crewe, UK).

Methods

Oligosaccharide preparation: Size-defined fractions of Na^+ heparin oligosaccharides were prepared by partial nitrous acid digestion of the parental polysaccharide followed by Superdex 30 chromatography as described previously.[45] The size and expected composition of the selected decasaccharide (DP-10) fragment was confirmed by comparison with authentic heparin standards on Superdex 30 and by PAGE, and by digestion with heparinases. The CS and KS oligosaccharides were extracted from bovine cartilage following papain digestion,[46] alkali treated and separated as previously described.[47]

Dual polarisation interferometry (DPI): DPI permits the direct measurement of changes in thickness, refractive index (RI) and mass of materials ≤ 100 nm thick on the surface of a glass waveguide in real time.[48] The dual-slab waveguide is illuminated with laser light of alternating polarisations at one end, and, as the light exits the two waveguides at the other end, they interfere to produce an interference pattern. The waveguide structure is integrated with a fluidic system permitting the continuous flow of material over the top waveguide, and, as material is added to or removed from the waveguide, the interference pattern moves, and these changes in the position of the interference pattern can be "resolved" into changes in thickness, RI and mass of the material on the waveguide.[49–51] Thus, if a protein is added to a heparin surface, the change in measured thickness will reflect the orientation the protein layer adopts on the surface. In addition there will be a surface coverage value (in $ng\,mm^{-2}$) and a refractive index measurement that will reflect the density of protein packing on the oligosaccharide surface.

All DPI measurements were performed on an *Ana*Light® Bio200 (Farfield Group, Crewe, UK) equipped with a 632.8 nm laser. The instrument is a dual-channel system, with each 2 μL cell maintained at 20 °C unless otherwise stated. Following calibration steps to measure the refractive index of the waveguide and running buffer, stepwise injections of materials over the waveguide to formulate the oligosaccharide surface were undertaken.

In situ formation of oligosaccharide surfaces: The following oligosaccharide surfaces were produced, keratan sulfate (KS), chondroitin sulfate (CS) and Na^+ heparin surfaces with a range of degrees of polymerisation (DP), from DP-4 (tetrasaccharide) up to DP-20. A glass waveguide sensor surface covalently functionalised with thiol groups was mounted in the dual polarisation interferometer instrument, and PBS was allowed to flow over the waveguide surface at a rate of 50 $\mu L\,min^{-1}$ in the case of the surface to be functionalised with heparin, while HEPES (10 mM) with the metal cations Mg, Mn and Ca (all at 2 mM) was used for reactions with CS and KS oligosaccharides. In other words, no divalent cations were present in the reactions of heparin and protein as they are not required for these interactions.

Once the baseline sensor response had stabilised, ethanol/water (80%, *w*/*w*) was allowed to flow over the sensor for 90 s, followed by PBS; this allowed the baseline to stabilise once again (this procedure was repeated as necessary to ensure that any trace surface contamination was removed and was typically achieved within 5 min). Pure water was injected for 90 s to allow the waveguide structure to be calibrated and to determine the refractive index of the buffer solution (given that the refractive index of 80% ethanol and pure water is known); the instrument response can be used to calculate the thickness and refractive index of the waveguide and the refractive index of the buffer solution (bulk refractive index) to be used in subsequent layer calculations.[50]

The flow cell temperature was then set to 30 °C, the flow rate was reduced to 10 $\mu L\,min^{-1}$, and BMPH (5 $mg\,mL^{-1}$, dissolved in PBS just prior to injection) was allowed to flow over the sensor for 15 min, then PBS was used to rinse the sensor for 10 min. Next, the oligosaccharide was dissolved in PBS adjusted to pH 5 (acetate was avoided as it was shown to adsorb to the thiol surface) and injected into only one of the two flow cells at a rate of 2 $\mu L\,min^{-1}$ for 100 min. Oligosaccharides that were not bound after 100 min were removed by washing the surface with PBS at 50 $\mu L\,min^{-1}$ for 10 min.

Blocking the unreacted hydrazide groups and creation of a control flow cell: Unreacted hydrazide groups were blocked by the addition of CH_3O-$(EG)_{17}$-NH-CO-C_4H_8-CHO or "PEG-CHO" (20 $mg\,mL^{-1}$) dissolved in PBS (200 μL^{-1}) flowed over the flow cell at a rate of 2 μL min. This was repeated a second time to ensure complete blocking of the hydrazide surfaces. Thus, each of the glycochips described in the following sections was composed of two parts, one flow cell containing the BMPH linker, an oligosaccharide and

the PEG blocker, whilst the control flow cell was identical except for the absence of oligosaccharide, thereby creating side-by-side active (carbohydrate-containing) and control surfaces.

Protein challenges: Solutions of different proteins were injected over the surfaces at a flow rate of 50 $\mu L\,min^{-1}$. For the KS surfaces, the following proteins were tested: wheat germ-agglutinin from *Triticum vulgaris* (WGA, $M_W = 36$ kDa, main specificity *N*-acetyl-β-D-glucosamine), *Maackia amurensis* lectin (MAA, $M_W = 130$ kDa, which specifically recognises sialic acid residues) and lactoferrin from bovine colostrum. In addition, the following control (nonbinding) proteins were added: Con A from *Canavalia ensiformis* ($M_W =$ 104 kDa, main specificity α-mannose) and BSA. For the heparin chip, FGF-2 and lactoferrin were the test proteins. All the proteins injected over the KS chip were dissolved in HEPES/NaCl buffer with divalent metal ions (2 mM), whist those proteins injected over the heparin surfaces were dissolved in PBS.

Lectins such as Con A, WGA and MAA bind carbohydrates though a network of hydrogen bonds, hydrophobic interactions, van der Waals interactions and metal ion co-ordinations. Metal ions such as Mg^{2+} and Ca^{2+} can assist in the positioning of the amino acid residues to interact with the carbohydrates, but with few conformational changes taking place upon binding in either protein or carbohydrate. Thus, the divalent metal ions allow the protein to adopt the required conformation to bind to carbohydrates, and are not known to alter the conformation of the carbohydrates.

Acknowledgements

The authors thank the Biotechnology and Biological Sciences Research Council, the Human Frontiers Science Programme, the RCUK "Glycochips" programme and the North West Cancer Research Fund for financial support. They also wish to thank Dr. Gavin Brown and Dr. Bob Lauder of Lancaster University for their assistance with the surface development, and for the provision of KS and CS, respectively.

Keywords: biosensors · glycosaminoglycans · growth factors · heparin · lactoferrin

[1] E. A. Yates, C. J. Terry, C. Rees, T. R. Rudd, L. Duchesne, M. A. Skidmore, R. Levy, N. T. K. Thanh, R. J. Nichols, D. T. Clarke, D. G. Fernig, *Biochem. Soc. Trans.* **2006**, *34*, 427–430.
[2] A. Ori, M. C. Wilkinson, D. G. Fernig, *Front. Biosci.* **2008**, *13*, 4309–4338.
[3] M. Froesch, L. M. Bindila, G. Baykut, M. Allen, J. Peter-Katalinic, A. D. Zamfir, *Rapid Commun. Mass Spectrom.* **2004**, *18*, 3084–3092.
[4] J. F. Cipollo, A. M. Awad, C. E. Costello, C. B. Hirschberg, *J. Biol. Chem.* **2005**, *280*, 26063–26072.
[5] R. N. Rej, K. R. Holme, A. S. Perlin, *Carbohydr. Res.* **1990**, *207*, 143–152.
[6] T. R. Rudd, M. A. Skidmore, S. E. Guimond, M. Guerrini, C. Cosentino, R. Edge, A. Brown, D. T. Clarke, G. Torri, J. E. Turnbull, R. J. Nichols, D. G. Fernig, E. A. Yates, *Carbohydr. Res.* **2008**, *343*, 2184–2193.
[7] E. W. Adams, D. M. Ratner, H. R. Bokesch, J. B. McMahon, B. R. O'Keefe, P. H. Seeberger, *Chem. Biol.* **2004**, *11*, 875–881.
[8] O. Carion, J. Lefebvre, G. Dubreucq, L. Dahri-Correia, J. Correia, O. Melnyk, *ChemBioChem* **2006**, *7*, 817–826.
[9] M. Delehedde, M. Lyon, J. T. Gallagher, P. S. Rudland, D. G. Fernig, *Biochem. J.* **2002**, *366*, 235–244.
[10] W. G. Willats, S. E. Rasmussen, T. Kristensen, J. D. Mikkelsen, J. P. Knox, *Proteomics* **2002**, *2*, 1666–1671.
[11] B. T. Houseman, M. Mrksich, *Chem. Biol.* **2002**, *9*, 443–454.
[12] F. Fazio, M. C. Bryan, O. Blixt, J. C. Paulson, C. Wong, *J. Am. Chem. Soc.* **2002**, *124*, 14397–14402.
[13] M. A. Skidmore, S. J. Patey, N. T. Thanh, D. G. Fernig, J. E. Turnbull, E. A. Yates, *Chem. Commun.* **2004**, 2700–2701.
[14] S. Park, I. Shin, *Angew. Chem.* **2002**, *114*, 3312–3314; *Angew. Chem. Int. Ed.* **2002**, *41*, 3180–3182.
[15] D. M. Ratner, E. W. Adams, J. Su, B. R. O'Keefe, M. Mrksich, P. H. Seeberger, *ChemBioChem* **2004**, *5*, 379–382.
[16] B. T. Houseman, E. S. Gawalt, M. Mrksich, *Langmuir* **2003**, *19*, 1522–1531.
[17] O. Blixt, S. Head, T. Mondala, C. Scanlan, M. E. Huflejt, R. Alvarez, M. C. Bryan, F. Fazio, D. Calarese, J. Stevens, N. Razi, D. J. Stevens, J. J. Skehel, I. van Die, D. R. Burton, I. A. Wilson, R. Cummings, N. Bovin, C. H. Wong, J. C. Paulson, *Proc. Natl. Acad. Sci. USA* **2004**, *101*, 17033–17038.
[18] J. L. de Paz, D. Spillmann, P. H. Seeberger, *Chem. Commun.* **2006**, 3116–3118.
[19] E. Bengtsson, A. Aspberg, D. Heinegard, Y. Sommarin, D. Spillmann, *J. Biol. Chem.* **2000**, *275*, 40695–40702.
[20] U. Friedrich, A. M. Blom, B. Dahlback, B. O. Villoutreix, *J. Biol. Chem.* **2001**, *276*, 24122–24128.
[21] M. Rusnati, C. Urbinati, A. Caputo, L. Possati, H. Lortat-Jacob, M. Giacca, D. Ribatti, M. Presta, *J. Biol. Chem.* **2001**, *276*, 22420–22425.
[22] R. I. Osmond, W. C. Kett, S. E. Skett, D. R. Coombe, *Anal. Biochem.* **2002**, *310*, 199–207.
[23] J. E. Knobloch, P. N. Shaklee, *Anal. Biochem.* **1997**, *245*, 231–241.
[24] B. Mulloy, M. J. Forster, C. Jones, D. B. Davies, *Biochem. J.* **1993**, *293*, 849–858.
[25] B. Kannan, K. Castelino, F. F. Chen, A. Majumdar, *Biosens. Bioelectron.* **2006**, *21*, 1960–1967.
[26] B. H. Schneider, E. L. Dickinson, M. D. Vach, J. V. Hoijer, L. V. Howard, *Biosens. Bioelectron.* **2000**, *15*, 13–22.
[27] S. Tosatti, S. M. De Paul, A. Askendal, S. VandeVondele, J. A. Hubbell, P. Tengvall, M. Textor, *Biomaterials* **2003**, *24*, 4949–4958.
[28] Z. L. Zhi, A. K. Powell, J. E. Turnbull, *Anal. Chem.* **2006**, *78*, 4786–4793.
[29] J. Brock, *Immunol. Today* **1995**, *16*, 417–419.
[30] J. H. Nuijens, P. H. van Berkel, F. L. Schanbacher, *J. Mammary Gland Biol. Neoplasia* **1996**, *1*, 285–295.
[31] D. M. Mann, E. Romm, M. Migliorini, *J. Biol. Chem.* **1994**, *269*, 23661–23667.
[32] H. F. Wu, D. M. Monroe, F. C. Church, *Arch. Biochem. Biophys.* **1995**, *317*, 85–92.
[33] S. Zou, C. E. Magura, W. L. Hurley, *Comp. Biochem. Physiol. B* **1992**, *103*, 889–895.
[34] S. A. Moore, B. F. Anderson, C. R. Groom, M. Haridas, E. N. Baker, *J. Mol. Biol.* **1997**, *274*, 222–236.
[35] P. E. Mead, J. W. Tweedie, *Nucleic Acids Res.* **1990**, *18*, 7167.
[36] A. Pierce, D. Colavizza, M. Benaissa, P. Maes, A. Tartar, J. Montreuil, G. Spik, *Eur. J. Biochem.* **1991**, *196*, 177–184.
[37] K. Shimazaki, T. Tazume, K. Uji, M. Tanaka, H. Kumura, K. Mikawa, T. Shimo-Oka, *J. Dairy Sci.* **1998**, *81*, 2841–2849.
[38] L. Meagher, H. J. Griesser, *Coll. Surf. B, Biointerf.* **2002**, *23*, 125–140.
[39] G. Pejler, *Biochem. J.* **1996**, *320*, 897–903.
[40] I. El Yazidi-Belkoura, D. Legrand, J. Nuijens, M. C. Slomianny, P. van Berkel, G. Spik, *Biochim. Biophys. Acta Gen. Subj.* **2001**, *1568*, 197–204.
[41] A. Walker, J. E. Turnbull, J. T. Gallagher, *J. Biol. Chem.* **1994**, *269*, 931–935.
[42] S. J. Goodger, C. J. Robinson, K. J. Murphy, N. Gasiunas, N. J. Harmer, T. L. Blundell, D. A. Pye, J. T. Gallagher, *J. Biol. Chem.* **2008**, *283*, 13001–13008.
[43] A. E. Eriksson, L. S. Cousens, L. H. Weaver, B. W. Matthews, *Proc. Natl. Acad. Sci. USA* **1991**, *88*, 3441–3445.
[44] Y. Ke, M. C. Wilkinson, D. G. Fernig, J. A. Smith, P. S. Rudland, R. Barraclough, *Biochim. Biophys. Acta Gene Struct. Expression* **1992**, *1131*, 307–310.
[45] J. E. Turnbull, *Methods Mol. Biol.* **2001**, *171*, 141–147.
[46] T. N. Huckerby, J. M. Dickenson, G. M. Brown, I. A. Nieduszynski, *Biochim. Biophys. Acta Gen. Subj.* **1995**, *1244*, 17–29.
[47] G. M. Brown, T. N. Huckerby, I. A. Nieduszynski, *Eur. J. Biochem.* **1994**, *224*, 281–308.
[48] G. H. Cross, Y. T. Ren, N. J. Freeman, *J. Appl. Phys.* **1999**, *86*, 6483–6488.
[49] S. J. Biehle, J. Carrozzella, R. Shukla, J. Popplewell, M. Swann, N. Freeman, J. F. Clark, *Biochim. Biophys. Acta Mol. Basis Dis.* **2004**, *1689*, 244–251.

[50] G. H. Cross, A. A. Reeves, S. Brand, J. F. Popplewell, L. L. Peel, M. J. Swann, N. J. Freeman, *Biosens. Bioelectron.* **2003**, *19*, 383–390.

[51] J. Popplewell, N. Freeman, S. Carrington, G. Ronan, C. McDonnell, R. C. Ford, *Biochem. Soc. Trans.* **2005**, *33*, 931–933.

Received: October 21, 2008
Published online on April 9, 2009

